Oxidation of polystyrene aerosols by VUV-photolysis and/or ozone†

José Salas Vicente,‡[a] Juan López Gejo,§[a] Sonja Rothenbacher,[b] Sumalekshmy Sarojiniamma,¶[a] Eliso Gogritchiani,‖[a] Michael Wörner,[a] Gerhard Kasper[b] and André M. Braun*[a]**

Received 10th February 2009, Accepted 8th April 2009
First published as an Advance Article on the web 27th April 2009
DOI: 10.1039/b902749a

Aerosols of submicron polystyrene particles were oxidized by either vacuum-ultraviolet (VUV) irradiation in the presence of molecular oxygen (O_2) and/or by ozone (O_3). Different degrees of oxidation and oxidative degradation were reached by VUV-photolysis depending on radiant energy, O_2 and H_2O concentrations in the bulk gas mixture as well as on particle diameter. The same functionalization was obtained by exposing the aerosol to O_3, however, oxidation, in particular oxidative degradation, was less efficient. The evolution of hydroxyl and carbonyl functions introduced was quantified by ATR-FTIR spectroscopy of filtered particles, and oxidative degradation of the polymer particles was confirmed by determining size and number of aerosol particles before and after oxidation. Efficiency analyses are based on the results of an O_3 actinometry and on an evaluation of the rate of absorbed photons by the aerosol particles in function of their size.

1. Introduction

The preparation of functionalized polymer and polymer-composite nanoparticles is of primary interest in materials research, and corresponding development work already led to a number of applications, *e.g.* in the biochemical and medical domain including drug and enzyme carriers,[1] absorbents,[2] affinity bioseparators,[3] as well as in the optical and optoelectrical domains.[4]

Functionalized (*e.g.* sulfonated) polymer particles are mostly prepared by (micro-)heterogeneous (co-)polymerisation of monomer or oligomer substrates bearing the corresponding reactive groups[5,6] or by coating inorganic, *e.g.* metal oxide particles, with such polymers.[7] However, the production of a larger range of functionalized polymer or copolymer particles of defined size, composition and morphology is usually realized in two phases: (i) the production of the polymer or copolymer substrate (particle or coat of nanoparticulate inorganic material) and (ii) the functionalization of the native polymer. These processes are normally performed in batch reactions, and to our knowledge, there is no published work describing such functionalization processes in a continuous regime.

A continuous process might be realized in a cascade of reactors (i) to produce functionalized nanoparticles, and (ii) to perform a primary as well as subsequent functionalizations of the original polymer or polymer coated particles. The polymerization of aerosol nanodroplets of liquid monomers or mixtures of monomers in a continuous operating regime has long been described[8] and claimed for a technical application,[9] yet the examples of the patent cited are not very informative. The experimental results obtained so far by the authors confirm qualitatively that polymer nanoparticles might be produced by a vacuum ultraviolet-(VUV-)photochemical polymerization of aerosol droplets, but the development of such a process requires a detailed knowledge of the gas dynamics in a continuously operating reactor and, consequently, a very special reactor design.

The work presented here therefore is focused on the *primary functionalization* of previously prepared and commercially available polystyrene nanoparticles. VUV-photochemical oxidation was chosen to avoid any addition of chemicals to the reaction system during primary functionalization,[10–14] except water (H_2O) and molecular oxygen (O_2). Taking into account that VUV-photolysis of O_2 produces O_3, the latter was used alternatively for the thermal oxidation of the polymer nanoparticles.

Earlier work on the functionalization of polystyrene films revealed that the VUV-photolysis of polystyrene leads to C–C-bond homolysis (reaction (1)).[12–14] Due to the reduced mobility within the polymer bulk, the C-centered radicals generated may mainly recombine, but evidence for disproportionation and cross-linking was found in the absence of O_2. In the presence of O_2, peroxyl radicals are generated as key intermediates of the subsequent thermal reactions leading to hydroxyl and carbonyl and carboxyl groups (reactions (2), (3) and (4), respectively).

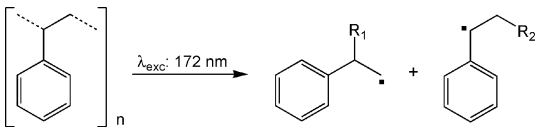

(1)

$$R^{\bullet} + O_2 \rightarrow RO_2^{\bullet} \quad (2)$$

[a]*Lehrstuhl für Umweltmesstechnik, Engler-Bunte-Institut, Universität Karlsruhe, Germany. E-mail: Andre.Braun@ciw.uni-karlsruhe.de*
[b]*Bereich Gas-Partikel-Systeme, Institut für Mechanische Verfahrenstechnik und Mechanik, Universität Karlsruhe, 76128, Karlsruhe, Germany*

† This article was published as part of the themed issue in honour of Esther Oliveros.

‡ Present address: UV-Consulting Peschl España S.L., 46980 Paterna (Valencia), Spain.
§ Present address: Departamento de Química Orgánica I, Universidad Complutense de Madrid, 28040 Madrid, Spain.
¶ Present address: School of Chemistry and Biochemistry, Georgia Institute of Technology, Atlanta, GA 30332, USA.
‖ Present address: Reuter Chemische Apparatebau KG, 79108 Freiburg, Germany.
** Present address: Institut für Bio- und Lebensmitteltechnik, IV. Molekulare Aufarbeitung von Bioprodukten, Universität Karlsruhe, 76128 Karlsruhe, Germany.

$$RO_2^{\bullet} \rightarrow\rightarrow ROH \rightarrow\rightarrow R'COH \rightarrow\rightarrow R'COOH \quad (3)$$

$$RR'CO_2^{\bullet} \rightarrow\rightarrow RR'C{=}O \quad (4)$$

VUV-photolysis of the gaseous bulk system containing O_2 generates atomic oxygen (O) (reaction (5)),[15] which is known to react from both triplet and singlet states with organic substrates by hydrogen abstraction (reaction (6)); the latter may also react by insertion into a C–H-bond (reaction (7)).[16,17] However, O predominantly adds to O_2 yielding ozone (O_3) (reaction (8)).[15]

$$O_2 + h\nu\,(\mathrm{VUV}) \rightarrow 2O \quad (5)$$

$$O + RH \rightarrow R^{\bullet} + HO^{\bullet} \quad (6)$$

$$O + RH \rightarrow ROH \quad (7)$$

$$O + O_2 \rightarrow O_3 \quad (8)$$

In the presence of H_2O, its VUV-photolysis may contribute to the oxidation of the polymer. In fact, the VUV-photolysis of H_2O (reaction (9)) is used to initiate the oxidation of organic compounds by intermediate hydroxyl ($HO^{\bullet}$) radicals *via* hydrogen abstraction (reaction (10)) and addition to π-systems (reaction (11)). Both reactions generate C-centered radicals[18] that are efficiently trapped by O_2 (reaction (2)). However, it was shown recently that $HO^{\bullet}$ generated in an aqueous bulk phase reacts very inefficiently with solid polymer surfaces,[19] and similar reactions in gas/solid heterogeneous systems cannot be competitive unless H_2O would be adsorbed on the aerosol particles when photolyzed.

$$H_2O + h\nu\,(\mathrm{VUV}) \rightarrow H^{\bullet} + HO^{\bullet} \quad (9)$$

$$HO^{\bullet} + RH \rightarrow R^{\bullet} + H_2O \quad (10)$$

$$HO^{\bullet} + RR'C{=}CR''R''' \rightarrow RR'C^{\bullet}{-}C(OH)R''R''' \quad (11)$$

$$R'COOH + HO^{\bullet} \rightarrow R'CO_2^{\bullet} + H_2O \quad (12)$$

$$R'CO_2^{\bullet} \rightarrow R'^{\bullet} + CO_2 \quad (13)$$

$HO^{\bullet}$ is also known to react with carboxylates and carboxylic acids by electron transfer and subsequent decarboxylation (reactions (12) and (13), respectively).[20]

Under the experimental conditions applied, the concentration of O_3, generated by the VUV-photolysis of the bulk gas phase containing O_2, remains small, and the effects of its VUV-photolysis on the overall reaction system are negligible. However, O_3 was found to react with solid polystyrene.[12,14,21] Alkanes are relatively inert to O_3,[22,23] and reaction products observed might either be explained by reactions of atomic oxygen (*vide supra*) or by reactive oxygen species generated in the presence of H_2O (reaction (14)) or hydrogen peroxide (H_2O_2, reaction (15)). In addition, oxidation and oxidative degradation might be enhanced by the generation (reaction (16)) and decay of ozonides (reaction (17)) and by reactions of O_3 with intermediates of VUV-photolyses (*e.g.* reactions (18), (16) as well as (1) and (19)).

$$O_3 + HO^{-} \rightarrow HO_2^{-} + O_2 \quad (14)$$

$$O_3 + HO_2^{-} \rightarrow HO^{\bullet} + O_2^{-\bullet} + O_2 \quad (15)$$

$$O_3 + HO_2^{\bullet} \rightarrow HO_3^{\bullet} + O_2 \quad (16)$$

$$HO_3^{\bullet} \rightarrow HO^{\bullet} + O_2 \quad (17)$$

$$H^{\bullet} + O_2 \rightarrow HO_2^{\bullet} \quad (18)$$

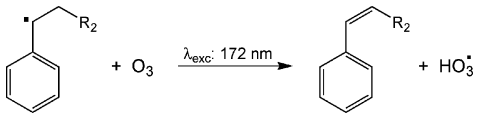

(19)

The oxidation of aromatic moieties by O_3 is thought to involve epoxidation and subsequent rearrangement to yield phenols.[24]

The aim of the present work was to check the feasibility of a continuous reaction system to functionalize polystyrene nanoparticles in the gas phase, before expanding the scope of such a process to more complex particle substrates (*e.g.* nanocomposites) and designing and combining reactors for gas and liquid phase reactions.[25] A differentiation between VUV-photochemical initiated oxidation and ozonolysis was made in order to evaluate the scope of application of the two processes.

2. Experimental part

2.1. Materials

Aqueous suspensions (approx. 10%) of polystyrene particles of different sizes (50, 98 and 500 nm; Surfactant Free Sulfate White Polystyrene Latex, Postnova Analitics, Germany), O_2 4.5, N_2 5.0 and synthetic air (Air Liquide, Germany) were used as purchased. H_2O was of tridistilled quality (UHQ-II).

2.2. Aerosol generation

250 μl of the aqueous suspensions of polystyrene particles of defined diameter (see section 2.1.) were diluted under stirring in 80 ml of distilled water. The highly diluted suspensions were fed into a Collison-Atomizer of defined diameter (Topas, ATM 220, Germany)[26] in which they were dispersed into the bulk gas phase by pressurized gas or gas mixtures (3 bar) (Fig. 1). Due to the high dilution, submicron droplets contained mostly (approx. 96%) one polystyrene particle. A deflector led bigger droplets back to the reservoir. Droplets were evaporated after passing the deflector by mixing the aerosol with heated dry gas mixtures.

2.3. VUV-photochemical oxidation of the polymer aerosol

The aerosol was led into an annular photochemical reactor that was equipped with a cylindrical Xe_2-excimer radiation source emitting at 172 (±14) nm and positioned in the central axis of the reactor. The radiation source (custom built) consisted of two concentric Suprasil® quartz tubes (length of discharge: 14 cm, outside diameter: 3.0 cm) with an inner electrode (phase) made of an aluminium foil and cooled with distilled water. The Xe_2-excimer radiation source was driven by a high voltage power supply (ENI, Model HPG-2) with electrical powers (P_e) of 20 to 150 W at 175 kHz. An additional Suprasil® tube (outside diameter: 3.8 cm) was positioned between the outer wall of the radiation source and the aerosol, providing a gap for the outer electrode. This outer electrode was made of an extensible net of stainless

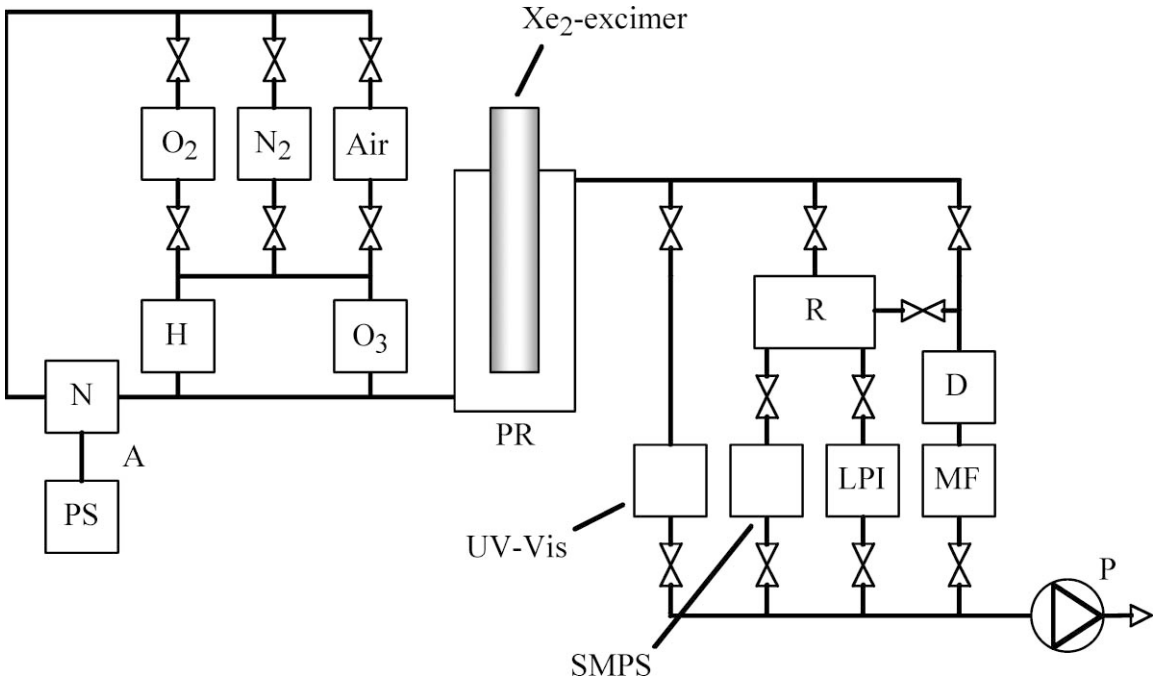

Fig. 1 Experimental set-up for aerosol generation, functionalization and analysis. *Aerosol generation*: A: atomizer, N: nozzles, PS: polystyrene suspension, H: gas heating system, O_3: ozonizer, O_2, N_2, Air: pressure bottles with respective gases. *Functionalization unit*: PR: photochemical reactor. *Analytical devices*: UV-Vis spectrophotometer, SMPS: scanning mobility particle sizer, R: agglomeration reservoir, LPI: low pressure impactor, D: charcoal denuder, MF: membrane filtration, P: vacuum pump.

steel (wire diameter: 0.1 mm) and was connected to the ground. The gap between the two Suprasil® tubes was purged with N_2 to avoid filter effects by O_2. The reactor had an optical path (l) of 7 mm, measured between the outer Suprasil® tube and the reactor wall. The outer (grounded) electrode could be covered partially with a metallic sheet. This variation of the length (d) of the irradiated annular volume allowed the control of the rate of incident photons ($P_{0,172}$). The maximum value of d was 140 mm. The reactor temperature was not controlled but reached a stable working temperature of approx. 60 °C.

2.4. Oxidation of the polymer aerosol by ozone

The aerosol of the native particles was mixed at the entrance of the photochemical reactor with O_3 (5×10^{-6} M in synthetic air) produced by an ozonizer (Sander, Germany). The ozonizer contained 7 water cooled elements of silent discharge that could be operated at 7 to 7.5 kV with a maximum electric power (P'_e) of 80 W. P'_e could be varied in % of the maximum value (see Fig. 10).

2.5. Analytic procedures

2.5.1. Actinometry. The rate of incident photons ($P_{0,172}$ [einstein s^{-1}]) was determined by O_3 actinometry[27,28] using synthetic air (estimated limit of error: ±5%). In-line ozone analyses were performed spectrophotometrically (Fig. 1, HP Spectrophotometer, 8452 DAD, Suprasil® spectroscopic cell (optical path: 1 cm, $\varepsilon_{O_3,258}$: 3000 M^{-1} cm^{-1}[29])).

The concentration of O_3 in the gaseous mixture ([O_3]) exiting the photochemical reactor increased with increasing P_e, but reached a level of saturation at $P_e \geq 150$ W (Fig. 2). It is interesting to note that addition of H_2O did not affect [O_3]. It may therefore be assumed that reaction (14) as well as reaction (20) are negligible within this context.

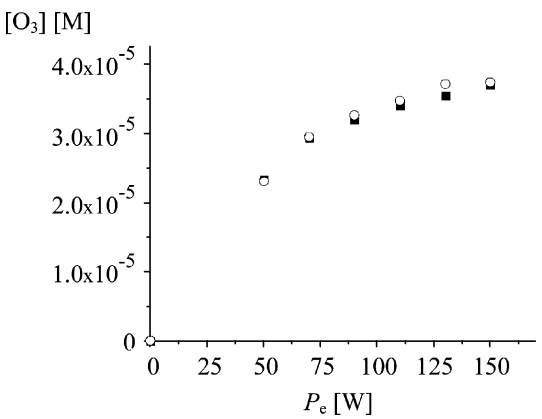

Fig. 2 O_3 production by VUV-photolysis of synthetic air. Concentration of O_3 [M] in the gaseous mixture exiting the photochemical reactor in function of the electric power of the Xe_2-excimer radiation source. Photolysis of dry synthetic air (■), addition of 3.6 mg L^{-1} of H_2O (○); flux: 7 L min^{-1}. Optical path: 7 mm; length of irradiated zone (d): 140 mm.

$$O + H_2O \rightarrow 2HO^{\bullet} \quad (20)$$

The Xe_2-excimer radiation source was not operational at $P_e <$ 20 W, and $P_e \geq 50$ W were chosen to obtain stable [O_3] for analytic purposes. Under the experimental conditions described in Fig. 2, $[O_3] = f(P_e)$ was found within a nonlinear domain. Under conditions of quasi-constant absorption during the time of actinometer photolysis, $[Pr]_{Ac}$ depends on $P_{a,\lambda}$ and on t (eqn (21)[30])

$$[Pr]_{Ac} = P_{0,\lambda}(1 - 10^{-\varepsilon_{Ac,\lambda}l[Ac]})\Phi_{Ac,\lambda}t = P_{a,\lambda}\Phi_{Ac,\lambda}t = Q_a\Phi_{Ac,\lambda} \quad (21)$$

where:

• $[Pr]_{Ac}$: concentration of product formed by the photolysis of the actinometer during time t [M]

• $\Phi_{Ac,\lambda}$: quantum yield of actinometric reaction

• $\varepsilon_{Ac,\lambda}$: molar absorption coefficient of actinometer [M^{-1} cm^{-1}]

• l: optical path [cm]

• [Ac]: concentration of actinometer [M]

• $P_{a,\lambda}$: rate of absorbed photons [einstein s^{-1}]

• t: time of photolysis [s]

• Q_a: absorbed photon energy [einstein].

The result depicted in Fig. 2 could be due to a nonlinear relation of $P_{0,172} = f(P_e)$ and/or to too high values of Q_a. The latter would lead to levels of $[O_3]$ where the VUV-photolysis of O_3 has to be taken into account and a quasi-steady state $[O_3]$ would eventually be reached. Both factors can be controlled by working at lower but constant values of P_e and by diminishing and varying t. In a continuous regime

$$t = \tau, \tag{22}$$

where τ is the residence time within the irradiated volume of the reactor [s], the residence time can be changed by varying either the flux of the gaseous reaction mixture (F) or the length of the irradiated volume (d). The latter does not involve changes of the flow characteristics and was implemented by inserting precisely cut metallic sheets into the gap provided for the outer (grounded) electrode (section 2.3.). A linear increase of $[O_3]$ in function of d with a slope of 1.9 (±0.2) × 10^{-7} M mm^{-1} was obtained for P_e = 50 W (Fig. 3).

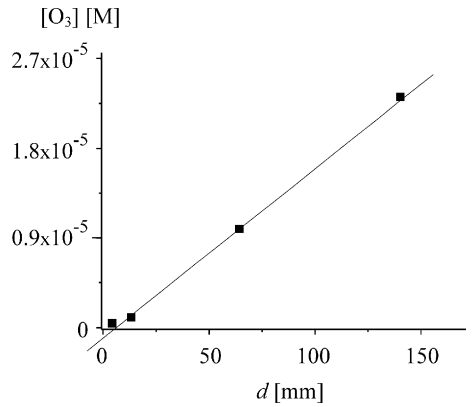

Fig. 3 O_3 production by VUV-photolysis of O_2. $[O_3]$ [M] in the gaseous mixture exiting the photochemical reactor as a function of d. F: 7 L min^{-1}. P_e: 50 W.

Based on eqn (21) and using the production of O_3 by VUV-photolysis of O_2 as an actinometer in a continuous regime, $P_{0,172}$ for a given reactor configuration is calculated with eqn (23)

$$P_{0,172} = \frac{[O_3]F}{\phi_{O_3,172}(1 - 10^{-\varepsilon_{O_2,172} l [O_2]})} \frac{n!}{r!(n-r)!} \tag{23}$$

where:

• $[O_3] = [Pr]_{Ac}$

• $\phi_{O_3,172}$: apparent quantum yield of O_3 production.

Whereas $\Phi_{O_3,172} = 2$, $\phi_{O_3,172}$ takes into account the main decay reactions of O_3, and the experimental eqn (24) was proposed for a most adequate fit.[31]

$$\phi_{O_3,172} = \phi_{O_3,172} - 1.10\frac{[O_3]}{[O_2]} \tag{24}$$

However, for $[O_3]/[O_2] < 10^{-2}$, $\Phi_{O_3,172} = 2$ was used. In earlier work of VUV-photochemical oxidations in the gas phase, total absorption by O_2 at 172 nm was found for l = 2.2 cm,[32] hence, for l = 7 mm, a calculated absorption $A_{172} = 0.62$ was applied. Since $A = \log(1/T)$, eqn (23) may be rewritten

$$P_{0,172} = \frac{[O_3]F}{\phi_{O_3,172} 0.76} \tag{25}$$

$P_{0,172}$ was related to P_e, and the corresponding values are given in Fig. 4 for d = 4 and 140 mm, respectively. For reasons already mentioned, $P_{0,172}$ was only assessed within the range of P_e shown in the graph. For d = 4 mm, a quasi-linear relation $P_{0,172} = f(P_e)$ was found with a slope of 3.3 × 10^{-9} einstein s^{-1} W^{-1} corresponding to a radiation efficiency of the Xe_2-excimer radiation source of 3.8%.

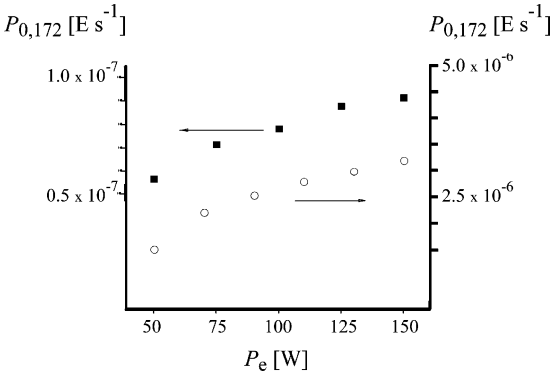

Fig. 4 VUV-photolysis of O_2 (synthetic air). $P_{0,172}$ in function of P_e for d = 4 mm (●) and d = 140 mm (○). l: 7 mm, F: 7 L min^{-1}.

2.5.2. Sampling for off-line analyses. Aerosol particles were filtered after passing the photochemical reactor unit (Teflon-membrane filter, pore size: 0.2 μm (Pall GmbH, Germany). An upstream denuder filled with charcoal was used to reduce ozononlysis of the accumulating particles during sampling time.

2.5.3. FTIR-Spectroscopy. Hydroxylation and carbonylation of the polymer particle surfaces were monitored with a Bruker Golden Gate® Diamond ATR Unit mounted on a Bruker Equinox® 55 FTIR spectrometer (resolution: 3 cm^{-1}, 60 scans per measurement). Fig. 5 shows the spectra of filtered polystyrene nanoparticles before and after irradiation and indicates the spectral domains used for quantification.

The evolution of the particle functionalization was determined in introducing an oxidation index ($I_{ox(fg)}$) that normalizes the integrated absorption band of either one of the oxygen containing functional groups (*e.g.* carbonyl) with reference to the absorption band of carbon–carbon double bonds that was relatively little or slightly inversely affected by the oxidation process (*e.g.* eqn (26)).[12–14,33]

$$I_{ox(C=O)} = \frac{\int \mathrm{Abs}(t)_{C=O}}{\int \mathrm{Abs}(t)_{ref}} - \frac{\int \mathrm{Abs}(0)_{C=O}}{\int \mathrm{Abs}(0)_{ref}} \tag{26}$$

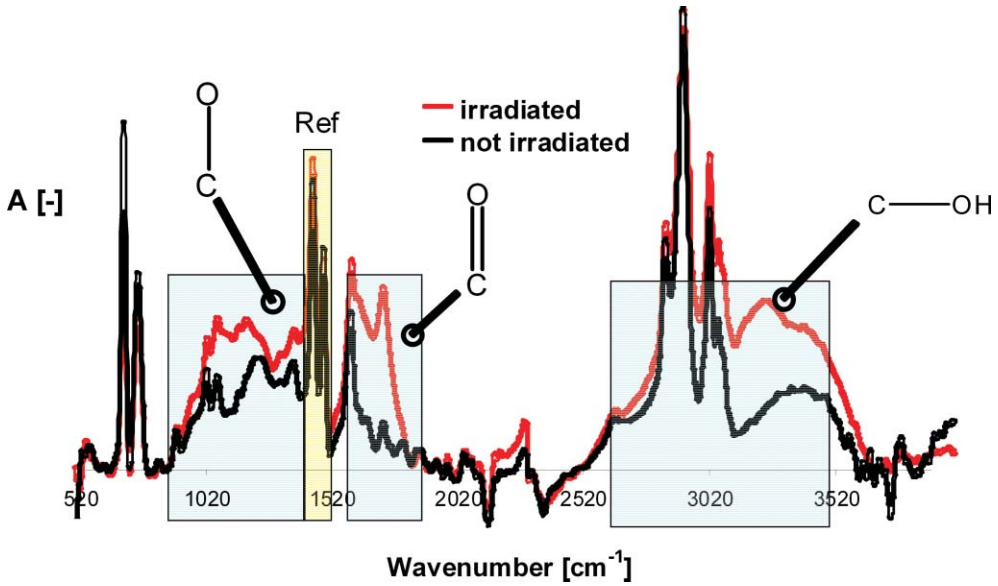

Fig. 5 FTIR-spectra of polystyrene particles before and after VUV-photochemical oxidation. Wavenumber regions of oxygen containing functional groups (blue) and of reference peaks (yellow) for the calculation of oxidation indices $I_{ox(fg)}$ are shown.[33]

where:

- $Abs(t)_{C=O}$: absorbance of C=O (1615–1840 cm^{-1}) at reaction time t
- $Abs(t)_{ref}$: absorbance of reference peaks (1471–1522 cm^{-1}) at reaction time t
- $Abs(0)_{C=O}$: absorbance of C=O (1615–1840 cm^{-1}) for unmodified polystyrene
- $Abs(0)_{ref}$: absorbance of reference peaks (1471–1522 cm^{-1}) for unmodified polystyrene.

2.5.4. Particle concentration and size distribution. After VUV-photochemical oxidation, the aerosol was led through a reservoir of 120 L to ensure equilibrium of the agglomeration–dissociation processes. A scanning particle mobility sizer (SMPS) was installed, consisting of a differential mobility analyzer (DMA; TSI Inc., USA, Model 3071), operating at 0.3 L min^{-1} of aerosol flow and 3.0 L min^{-1} of sheath air, and a condensation particle counter (CPC; TSI Inc., USA, Model 3022).

3. Results and discussion

As expected from the results of foregoing experiments with polystyrene films,[12–14] the VUV-irradiation of polystyrene aerosol particles led primarily to the oxidation of their surfaces,[10] where carbonyl and hydroxyl functions were formed (Fig. 5), The evolution of $I_{ox(C=O)}$ as a function of the concentration of O_2 in the gaseous bulk phase and of P_e of the Xe_2-excimer lamp is shown in Fig. 6.

The result confirms the mechanistic hypothesis already derived from the work with polystyrene films[12–14] that VUV-photochemical C–C bond homolysis is the main reaction path leading to the oxidation of polystyrene. At higher O_2 concentration, the increased absorption cross-section of the bulk gas phase leads to a decrease of polystyrene photolysis and therefore to lower oxidation indices for comparable energy inputs. Alternatively, assuming that photochemically generated $HO^{\bullet}$ or O would primarily initiate the oxidation, the short lifetimes of these intermediates would require their generation close to the surface of the particles, and the same explanation would hold. Given the fact that, for a given mass of aerosol particles, the part of reflected radiation decreases with decreasing diameter (*vide infra*), the result shown in Fig. 6b was to be expected.

$I_{ox(C=O)}$ reached a limiting value of approx. 1.6 for different incident radiant energies (Q_e) depending on the particle diameter (Fig. 7) and on the O_2 concentration in the gaseous bulk phase.

Based on these results, the rate of absorbed photons ($P_{a,172}$) and the absorbed radiant energy (Q_a) could be evaluated for related experiments. For this purpose, $P_{0,172}$ was differentiated into scattered ($P_{s,172}$), absorbed ($P_{a,172}$) and transmitted ($P_{t,172}$) rates of photons (eqn (27)), and results were taken from experiments, where $Q_{0,172}$ = constant.

$$P_{0,172} = P_{a,172,2r} + P_{s,172,2r} + P_{t,172,2r} \tag{27}$$

where:

- $P_{a,172,2r} = P_{0,172}(1 - e^{-\rho\sigma_{172}l})$
- ρ: number density of particles [m^{-3}]
- σ_{172}: absorption cross section [m^2]
-

$$P_{s,172,2r} = P_{0,172}\,(1 - e^{-\rho\sigma_{s,172}l})\,^{34} \tag{28}$$

- $\sigma_{s,172}$: scattering cross section [m^2].

Assuming that $P_{t,\lambda}$ could be neglected, $P_{a,172}$ is calculated as the difference

$$P_{a,172,2r} = P_{0,172} - P_{s,172,2r} = P_{0,172} - (P_{0,172}(1 - e^{-\rho\sigma_{s,172}l})) \tag{29}$$

and for very dilute suspensions, the exponential factor may be replaced

$$\begin{aligned} P_{a,172,2r} &= P_{0,172} - P_{s,172,2r} = P_{0,172} - P_{0,172}\rho\sigma_{s,172}l \\ &= P_{0,172}(1 - \rho\sigma_{s,172}l) \end{aligned} \tag{30}$$

Expressing ρ in terms of mass per unit volume,

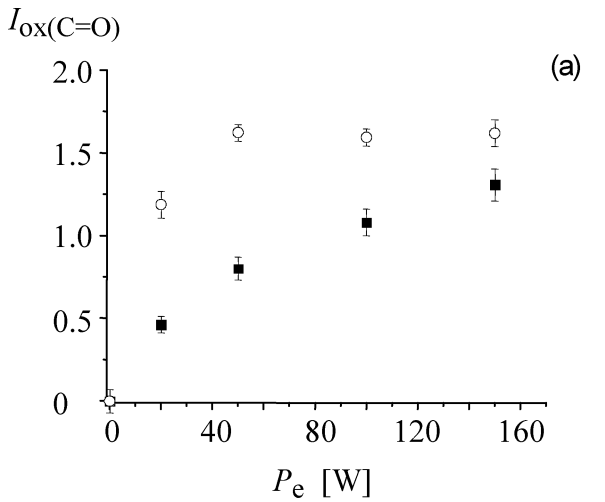

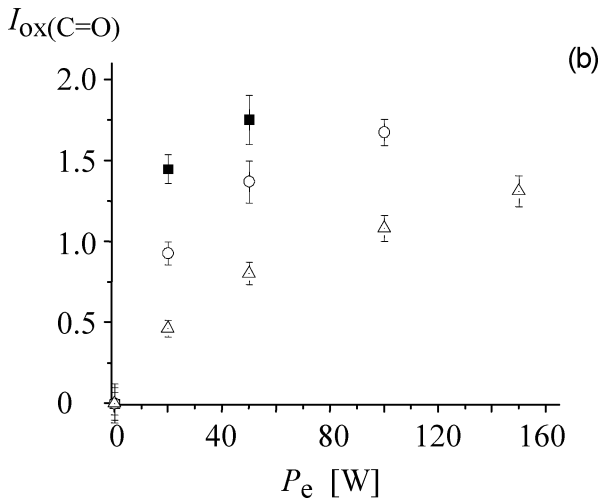

Fig. 6 VUV-photochemical oxidation of an aerosol of polystyrene particles. Evolution of the oxidation index $I_{ox(C=O)}$ in function of the electric power of the Xe_2-excimer lamp (P_e) and depending on (a) the concentration of O_2 in the gaseous bulk phase and (b) the aerosol particle diameter ($2r$). The polystyrene aerosol was produced by spraying an approx. 0.3 g L^{-1} aqueous suspension of particles of defined diameter into a heated gas stream (pressure at the atomizer: 3 bar); F: 7 L min^{-1}; temperature (T): approx. 60 °C. (a) $2r$: 500 nm; composition of gaseous bulk phase: O_2: 8.5% (○), 20% (■), H_2O: evaporating from the aerosol droplets, approx. 0.5%, N_2: difference to 100%. (b) Composition of gaseous bulk phase: O_2: 20%, H_2O: evaporating from the aerosol droplets, approx. 0.5%, N_2: difference to 100%; $2r$: 50 nm (■), 98 nm (○), 500 nm (△).

$$\rho'_{s,172} = \frac{V_R \delta}{S_p l} \tag{31}$$

where

- V_R: volume of reactor [m^3]
- δ: density of polystyrene (1020 kg m^{-3})
- S_p: surface of projection of particles [m^3]

eqn (30) may be written as

$$P_{a,172,2r} = P_{0,172}\left(1 - \frac{V_R \delta}{S_p l}\sigma_{s,172} l\right) = P_{0,172}\left(1 - \frac{V_R \delta}{\pi r^2}\sigma_{s,172}\right) \tag{32}$$

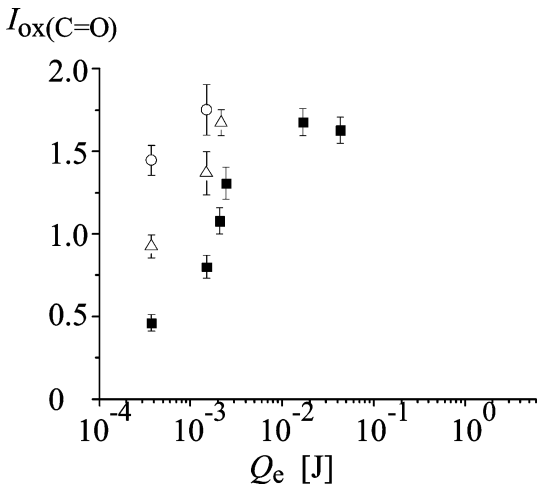

Fig. 7 VUV-photochemical oxidation of an aerosol of polystyrene particles. Evolution of the oxidation index $I_{ox(C=O)}$ in function of the incident radiant energy (Q_e) and depending on the aerosol particle diameter ($2r$). The polystyrene aerosol was produced by spraying an approx. 0.3 g L^{-1} aqueous suspension of particles of defined diameter into a heated gas stream (pressure at the atomizer: 3 bar); F: 7 L min^{-1}; T: approx. 60 °C; composition of gaseous bulk phase: O_2: 20%, H_2O: evaporating from the aerosol droplets, approx. 0.5%, N_2: difference to 100%; $2r$: 50 nm (○), 98 nm (△), 500 nm (■).

$P_{s,172,2r}$ was also related to the differential scattering cross section C'_s,[35]

$$P'_{s,172,2r} = P_{0,172}\frac{1}{r^2}C'_{s,172} \tag{33}$$

and after integrating C'_s over the whole sphere of observation,

$$P_{s,172,2r} = P_{0,172}\frac{1}{r^2}\int_{4\pi}\frac{C'_{s,172}}{d\Omega} = P_{0,172}\frac{1}{r^2}4\pi C'_{s,172} = P_{0,172}\frac{1}{r^2}\sigma_{s,172} \tag{34}$$

the combination of eqn (30) and (34) yields

$$P_{a,172,2r} = P_{0,172}\left(1 - \frac{1}{r^2}\sigma_{s,172}\right) \tag{35}$$

Values of $\sigma_{s,172}$ could not be found in the literature and were calculated using eqn (36)[34] (see Table 1).

$$\sigma_{Ray} = \frac{8\pi}{3}\left(\frac{2\pi n_{med}}{\lambda_0}\right)^4 a^6\left(\frac{m^2-1}{m^2+2}\right)^2 \tag{36}$$

where

- λ_0: wavelength of incident radiation [m]
- a: particle radius (r) [m]

Table 1 Calculated $\sigma_{Ray,172}$ depending on the $2r$ of the polystyrene particles used and the corresponding $P_{s,172,2r}$ and $P_{a,172,2r}$ calculated (eqn (31)) for experiments made with $P_e = 50$ W, $F = 7$ L min^{-1} and $d = 4$ mm ($P_{0,172} = 5.70 \times 10^{-8}$ einstein s^{-1})

$2r$/nm	$\sigma_{Ray,172}/m^2$	$P_{s,172,2r}$/ einstein s^{-1}	$P_{a,172,2r}$/ einstein s^{-1}	$\frac{P_{a,172,2r}}{P_{a,172,50}}$	$\frac{I_{ox(C=O),2r}}{I_{ox(C=O),50}}$
50	6.27×10^{-15}	3.23×10^{-10}	$5.67 \times 10^{-}$	1	1
100	4.01×10^{-13}	5.4×10^{-9}	5.16×10^{-8}	0.91	0.62
500	6.27×10^{-9}	3.23×10^{-6}	—		0.31

• $m = n_p/n_{med}$

• n_p: refractive index of the particle (1.59, ref. 34)

n_{med}: refractive index of the surrounding medium (1.0003).

The calculated value of $P_{s,172,500}$ exceeds $P_{0,172}$. The Rayleigh approximation (eqn (36)) being in fact not applicable for $2r \geq \lambda$,[34] $P_{s,172,500}$ is largely overestimated. Inversely, $P_{a,172,50}$ may be taken as a reference to compare normalized values $P_{a,172,2r}/P_{a,172,50}$ and $I_{ox(C=O),2r}/I_{ox(C=O),50}$. $I_{ox(C=O),100}/I_{ox(C=O),50}$, based on experimental results, exceeds the calculated $P_{a,172,100}/P_{a,172,50}$ by a factor of 3. The result is probably due to the vast manifold of oxidation reactions initiated by the VUV-photolyis of polystyrene leading in most cases to quantum yields of substrate oxidation (ϕ_{-S}) > 1. This kind of chain reaction might be enhanced in the presence of O_3, whereas ozonolysis of polystyrene was found to be of minor importance (*vide infra*).

The maximum level for $I_{ox(C=O)}$ (Fig. 7) represents an average surface concentration of carbonyl functions that apparently cannot be exceeded because of an ongoing oxidative degradation of the particles. In fact, Fig. 8 shows the diminutions of particle diameter (2*r*, Fig. 8a) and concentration (% c_p, Fig. 8b) depending on P_e, but in the latter case more strongly on τ. At short τ (F = 7 L min^{-1}), the maximum $I_{ox(C=O)}$ of 1.6 was obtained with a $P_e \geq 100$ W. Under these experimental conditions, the particles lost in average approximately 5% of their original diameter, and their concentration diminished by 2%. Short τ seem to be favourable for a slow loss of mass that is primarily controlled by an oxidative degradation of the particle surface. At higher τ, particle loss was much more pronounced than the diminution of their size, and these results indicate that, parallel to a continuous diminution of particle size, oxidation may lead to a disruption of the particles, the smaller fragments being oxidized at much higher rate. At high values of τ and P_e, only 20% of the original particle concentration ($c_{P,0}$) were left. It is interesting to note that the particle concentration diminished at highest rate in the absence of O_2, confirming the dominant impact of the VUV-photolysis and the competitive rate of depolymerization of polystyrene. A similar loss of material was already reported for the VUV-photochemical oxidative functionalization of polystyrene films.[12–14]

Styrene and unsaturated polymeric and/or oligomeric intermediate products were already observed by GC/MS analysis and fluorescence measurements (λ_{exc} > 350 nm), respectively, when polystyrene films were irradiated in the absence of O_2.[12,14] Styrene as a product of a competing depolymerization was also detected in the bulk gas phase during photooxychlorination experiments, where sufficient amounts of polymeric material could be treated.[25,36]

Under VUV-irradiation, photolysis of polystyrene was found to be the primary chemical reaction that leads in the presence of O_2, *via* oxidation and oxygenation of the intermediates, to hydroxylated and carbonylated products. This photochemically initiated oxidative functionalization is assumed to be accelerated by O_3, produced by the VUV-photolysis of the gaseous bulk phase containing O_2 (reactions (5) and (8)). Due to the relatively low concentration of O_3 generated by the VUV-photolysis of O_2, its photolysis may be neglected, but its contribution to the overall rate of polystyrene oxidation may involve the reaction manifold described in section 1. In addition, little is known about the efficiency of the oxidation of polystyrene exposed to O_3, whereas

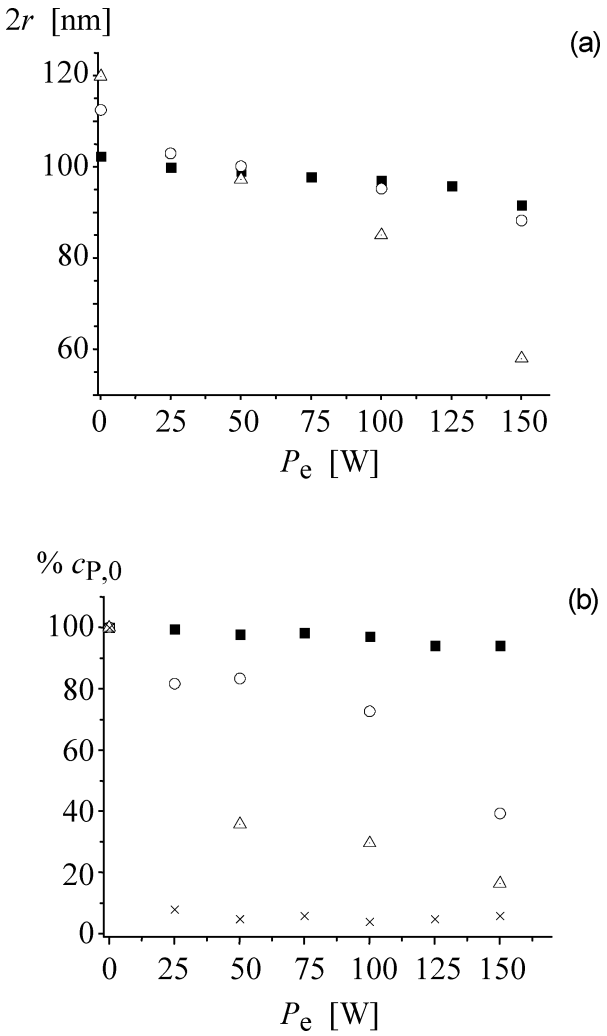

Fig. 8 VUV-photochemical oxidation of an aerosol of polystyrene particles of a diameter (2*r*) of 100 nm. Evolution of (a) particle diameter (2*r*) and (b) percent of initial particles (% $c_{P,0}$)) measured at the exit of the photochemical reactor depending on P_e and on τ. The latter is represented by F: 7 L min^{-1} (■), 3 L min^{-1} (○), 0.3 L min^{-1} (△). Polystyrene aerosol produced by spraying an approx. 0.3 g L^{-1} aqueous suspension of particles into a heated gas stream; *d*: 140 mm; pressure at the atomizer: 3 bar; composition of gaseous bulk phase: O_2: approx. 20%, H_2O: evaporating from the aerosol droplets, approx. 0.5%, N_2: difference to 100%; temperature: approx. 60 °C. Percent of initial particles measured in the absence of O_2 is shown for comparison: F: 7 L min^{-1} (×).

the UV/O_3-technology was identified quite early as a convenient means of polymer particle functionalization.[37]

In order to investigate the ozonolysis of polystyrene aerosols, O_3 was produced from synthetic air by an ozonizer. The minimum ozone concentration ([O_3]) that could be maintained during several hours was 5×10^{-6} M. For comparison, a steady [O_3] of 8.6 (± 0.5) $\times 10^{-7}$ M was found under conditions, where the Xe_2-excimer radiation source (P_e = 150 W, d = 4 mm) irradiated synthetic air containing 0.5% of H_2O at F = 7 L min^{-1} (Fig. 9).

The evolution of $I_{ox(C=O)}$ with the time of ozonolysis is depicted in Fig. 10 for particles of $2r$ = 500 nm. As already observed with polymer films, the increase of $I_{ox(C=O)}$ was found to be quasi-linear, and in the case of the aerosol particles, a slope of

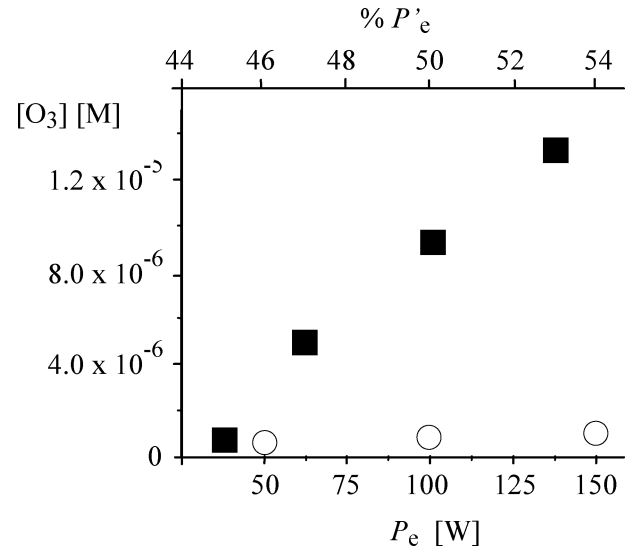

Fig. 9 O_3 production by ozonizer (■) and by VUV-photolysis (○) using synthetic air containing 0.5% of H_2O, F: 7 L min^{-1}. Measured O_3 concentrations ([O_3]) [M] in function of the electric powers of the ozonizer (P'_e, see experimental details) and of the Xe_2-excimer radiation source (P_e) with d: 4 mm).

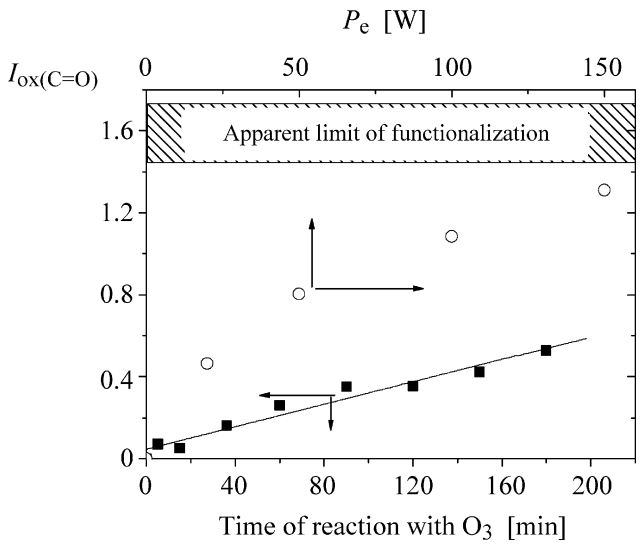

Fig. 10 Oxidation of an aerosol of polystyrene particles (2r: 500 nm) in synthetic air containing 5% of H_2O by VUV-photolysis and/or by O_3. Polystyrene aerosol produced by spraying an approx. 0.3 g L^{-1} aqueous suspension of particles into a heated gas stream (pressure at the atomizer: 3 bar), F: 7 L min^{-1}. (○) Evolution of the oxidation index $I_{ox(C=O)}$ in function of P_e; τ: 1.56×10^{-2} s, temperature: approx. 60 °C; time of exposure to O_3: approx. 1.7 s. (■) Evolution of the oxidation index $I_{ox(C=O)}$ in function of time of reaction with a steady $[O_3] = 5 \times 10^{-6}$ M.

4.8 (±0.3) × 10^{-5} s^{-1} was determined. It is also interesting to note that the same value of $I_{ox(C=O)}$ was found when the polystyrene particles were placed on a filter and ozonized for the same period of time. Using polystyrene particles of the same diameter, the VUV-photochemical experiment ($\tau = 1.56 \times 10^{-2}$ s) led to a value of $I_{ox(C=O)}$ of 1.3 (Fig. 6b and 10). Functionalization by the combination of a VUV-photochemically initiated oxidation and ozonolysis of polystyrene is therefore by at least a factor 100 more efficient than ozonolysis alone. Nevertheless, the latter might be used advantageously for a strictly controlled functionalization process without notable oxidative degradation.

4. Conclusion

VUV-photolysis of aerosols of polystyrene particles initiated their oxidation to different degrees of surface functionalization depending on radiant energy, O_2 and H_2O concentrations of the bulk gas mixture and particle diameter. The evolution of hydroxylation and carbonyl functions produced was quantified by FTIR-spectroscopy of filtered particles after defining an index of oxidation ($I_{ox(fg)}$). Functionalization could not exceed a given value independent of the particle diameter (*e.g.* $I_{ox(C=O)} \leq 1.6$), most probably due to the oxidative degradation of the polymer particles. Oxidative degradation of the polymer material, leading to a diminution of particle size and concentration, occurred in parallel, and optimum conditions for a given degree of oxidative functionalization at minimum alteration of the morphologic characteristics of the particles would have to be found. The same functionalization, but with much less efficiency, was also obtained by exposing the aerosol to O_3. This thermal oxidation allows a controlled functionalization to smaller values of $I_{ox(fg)}$ without notable oxidative degradation. VUV-photolysis of O_2 producing O_3 in a defined flux of synthetic air was used as an actinometer to relate the electric power of the Xe_2-excimer lamp (P_e) to its emitted radiant power ($P_{0,172}$), and, based on an approximation of the scattering cross-section for the wavelength of the incident radiation (172 nm), the rate of photons absorbed by the particles was evaluated for particle diameters ≤ 100 nm.

Acknowledgements

The authors acknowledge financial support by the Deutsche Forschungsgemeinschaft (DFG) and the Landesstiftung Baden-Württemberg.

References

1 J. Fu, J. Fiegel and J. Hanes, Synthesis and characterization of PEG based ether-anhydride terpolymers: New polymers for controlled drug delivery, *Macromolecules*, 2004, **37**, 7174–7180.
2 See, for example: J.-Y. Kim, J. Wainaina, J.-H. Kim and J.-K. Shim, Use of polymer nanoparticles as functional nano-absorbents for low-molecular weight hydrophobic pollutants, *J. Nanosci. Nanotechnol.*, 2007, **7**, 4000–4004.
3 S. Saliterman, *Fundamentals of BioMEMS and Medical Microdevices*, SPIE Press, Bellingham WA, 98225–6705, USA, 2006.
4 See, for example: I. Willner and B. Willner, Functional nanoparticle architectures for sensoric, optoelectronic and bioelectronic applications, *Pure Appl. Chem.*, 2002, **74**, 1773–1783.
5 See, for example: R. Jordan, N. West, A. Ulman, Y.-M. Chou and O. Nuyken, Nanocomposites by surface-initiated living cationic polymerization of 2-oxazolines on functionalized gold nanoparticles, *Macromolecules*, 2001, **34**, 1606–1611.
6 See, for example: C. Pichot, Position paper: functional polymer latexes, *Polym. Adv. Technol.*, 1995, **6**, 427–434.
7 See, for example: T. Dey, Polymer-coated magnetic nanoparticles: surface modification and end-functionalization, *J. Nanosci. Nanotechnol.*, 2006, **6**, 2479–2483.
8 (*a*) R. Pearson and G. Langer, Generation of aerosols by vapour-phase polymerization of methyl acrylate, *Nature*, 1960, **187**, 235; (*b*) R. Partch, E. Matijevi, A. W. Hodgson and B. E. Aiken, Preparation of polymer colloids by chemical reactions in aerosols. I. Poly,(*p*-tertiarybutylstyrene), *J. Polym. Sci., Polym. Chem. Ed.*, 1983, **21**, 961; (*c*) C. Esen and G. Schweiger, Preparation of Monodisperse Polymer

Particles by Photopolymerization, *J. Colloid Interface Sci.*, 1996, **179**, 276–280; (*d*) H. Morita, K. Semba, Z. Bastl, J. Subrt and J. Pola, N_2 laser-induced formation of copolymeric ultrafine particles in a gaseous tetraethenylgermane-carbon disulfide mixture, *J. Photochem. Photobiol., A*, 2005, **171**, 21–26.
9 D. Lösch, V. Seidl and M. Rübenacker, Process for production of polymer powders containing vinylformamide units, BASF AG, Publ. Nr. WO/2007/054442, Intl. Appl. No.: PCT/EP2006/067866, 08.11.2005.
10 A. Hozumi, H. Inagaki and T. Kameyama, The hydrophilization of polystyrene substrates by 172 nm vacuum ultraviolet light, *J. Colloid Interface Sci.*, 2004, **278**, 383–392.
11 V. M. Graubner, R. Jordan, O. Nuyken, B. Schnyder, T. Lippert, R. Kötz and A. Wokaun, Photochemical modification of cross-linked poly(dimethylsiloxane) by irradiation at 172 nmn, *Macromolecules*, 2004, **37**, 5936–5943.
12 J. López Gejo, *Applications of the VUV-photochemically initiated oxidation for waste gas treatment and surface functionalization*, Dissertation, Fakultät für Chemieingenieurwesen und Verfahrenstechnik, Universität Karlsruhe, Karlsruhe, 2005.
13 J. López Gejo, H. Glieman, T. Schimmel and A. M. Braun, Vacuum-ultraviolet photochemically initiated modification of polystyrene surfaces: chemical changes, *Photochem. Photobiol.*, 2005, **81**, 777–782.
14 J. López Gejo, N. P. Manoj, S. Sumalekshmy, H. Gliemann, T. Schimmel, M. Wörner and A. M. Braun, Vacuum-ultraviolet photochemically initiated modification of polystyrene surfaces: morphological changes and mechanistic investigations, *Photochem. Photobiol. Sci.*, 2006, **5**, 948–954.
15 See, for example: V. V. Ivanov, N. A. Popov, O. V. Proshina, T. V. Rakhimova, G. B. Rulev and V. B. Saenko, Study of the ozone production and loss during oxygen photolysis in a VUV-ozonator chamber, *Tech. Phys. Lett.*, 2001, **27**, 29–31.
16 C. S. Foote, J. S. Valentine and A. Greenberg, *Active Oxygen in Chemistry*, Springer, New York, 1995.
17 R. Wrobel, W. Sander, E. Kraka and D. Cremer, Reactions of dimethyl ether with atomic oxygen: a matrix isolation and a quantum chemical study, *J. Phys. Chem. A*, 1999, **103**, 3693–3705.
18 M. C. Gonzalez, E. Oliveros, M. Wörner and A. M. Braun, Vacuum ultraviolet photolysis of aqueous reaction systems, *J. Photochem. Photobiol., C*, 2004, **5**, 225–246.
19 M. Zahorodna, E. Oliveros, M. Wörner, R. Bogoczek and A. M. Braun, Dissolution and mineralization of ion exchange resins: differentiation between heterogeneous and homogeneous (photo-)Fenton processes, *Photochem. Photobiol. Sci.*, 2008, **7**, 1480–1492.
20 N. Quici, M. I. Litter, A. M. Braun and E. Oliveros, Vacuum-UV photolysis of aqueous solutions of citric and gallic acids, *J. Photochem. Photobiol., A*, 2008, **197**, 306–312.
21 W. Kern, Photochemical modification of polymer surfaces, *Trends Photochem. Photobiol.*, 2001, **7**, 11–30.
22 D. Feldman, *Polymeric Building Materials*, Taylor & Francis, Routledge, New York, 1989.
23 G. A. Olah and Á. Molnár, *Hydrocarbon Chemistry*, Wiley, New York, 2003.
24 V. D. Komissarov and I. N. Komissarova, Formation of phenol during ozonolysis of benzene, *Russ. Chem. Bull.*, 1973, **22**, 656–658.
25 J. Salas, *Vicente. Modificatión fotoquímica de submicropartículas en aerosoles*, Doctoral thesis, Universidad Politécnica de Valencia, Valencia, 2006 (Experimental work: Lehrstuhl für Umweltmesstechnik, Universität Karlsruhe).
26 K. R. May, The Collison nebulizer: description, performance and application, *J. Aerosol Sci.*, 1973, **4**, 235–238.
27 Zs. Laszló, I. Ilisz, G. Peintler and A. Dombl, VUV intensity measurement of a 172 nm Xe excimer lamp by means of oxygen actinometry, *Ozone: Sci. Eng.*, 1998, **20**, 421–432.
28 H. J. Kuhn, S. E. Braslavsky and R. Schmidt, Chemical actinometry, *Pure Appl. Chem.*, 2004, **76**, 2105–2146.
29 (*a*) G. Gordon, G. E. Pacey, W. J. Cooper and R. G. Rice, Current state-of-the-art measurements of ozone in the gas phase and in solution, *Ozone: Sci. Eng.*, 1988, **10**, 353–365; (*b*) K. Rakness, G. Gordon, B. Langlais, W. Masschelein, N. Matsumoto, Y. Richard, C. M. Robson and I. Somiya, Guideline for measurement of ozone concentration in the process gas from an ozone generator, *Ozone: Sci. Eng.*, 1996, **18**, 209–229.
30 (*a*) A. M. Braun, M.-T. Maurette and E. Oliveros, *Technologie photochimique*, Presses Polytechniques Romandes, Lausanne, 1986, Chapter 6.11; (*b*) A. M. Braun, M.-T. Maurette and E. Oliveros, *Photochemical Technology*, transl. D. F. Ollis and N. Serpone, Wiley, Chichester, 1991, Chapter 6.11.
31 Z. Falkenstein, Ozone formation with (V)UV-enhanced dielectric barrier discharges in dry and humid gas mixtures of O_2, N_2/O_2, and Ar/O_2, *Ozone: Sci. Eng.*, 1999, **21**, 583–603.
32 A. M. Braun, I. Gassiot Pintori, H.-P. Popp, Y. Wakahata and M. Wörner, Technical development of UV-C- and VUV-photochemically induced oxidative degradation processes, *Water Sci. Technol.*, 2004, **49**, 235–240.
33 J. Salas Vicente, J. López Gejo, S. Rothenbacher, S. Sarojiniamma, E. Gogritchiani, M. A. Miranda, M. Wörner, E. Oliveros, G. Kasper and A. M. Braun, VUV-photochemical functionalization of polystyrene aerosols, in *Basics and applications of photopolymerization reactions*, ed. J. P. Fouassier and X. Allonas, Research Signpost, Trivandrum, India, 2009.
34 A. J. Cox, A. J. DeWeerd and J. Linden, An experiment to measure Mie and Rayleigh total scattering cross sections, *Am. J. Phys.*, 2002, **70**, 620–625.
35 D. W. Hahn, *Light scattering theory*, University of Florida, Gainesville, 2008, http://plaza.ufl.edu/dwhahn/Rayleigh%20and%20Mie%20Light%20Scattering.pdf.
36 J. Salas Vicente, J. López Gejo, S. Rothenbacher, M. Wörner, E. Oliveros, G. Kasper and A. M. Braun, Functionalization of polystyrene aerosol particles by photooxychlorination, *Appl. Mater. Interface*, in preparation.
37 G. V. Lubarsky, M. R. Davidson and R. H. Bradley, Characterization of polystyrene microspheres surface-modified using a novel UV-ozone/fluidized- bed reactor, *Appl. Surf. Sci.*, 2004, **227**, 268–274.

